

First-principles study of the structural, elastic, and electronic properties of the cubic perovskite BaHfO₃

Hongsheng Zhao^{1,2,3}, Aimin Chang¹‡ and Yunlan Wang⁴

¹ Xinjiang Technical Institute of Physics and Chemistry, Chinese Academy of Sciences, Urumqi 830011, P.R.China

² Institute of Semiconductors, Chinese Academy of Sciences P.O.Box 912, Beijing 100083, P.R.China

³ Graduate School of Chinese Academy of Sciences, Beijing 100049, P.R.China

⁴ Center for High Performance Computing, Northwestern Polytechnical University, Xi'an 710072, P.R.China

E-mail: zhaohscas@yahoo.com.cn

Abstract. First principles study of structural, elastic, and electronic properties of the cubic perovskitetype BaHfO₃ has been performed using the plane wave ultrasoft pseudo-potential method based on density functional theory with revised Perdew-Burke-Ernzerhof exchange-correlation functional of the generalized gradient approximation (GGA-RPBE). The calculated equilibrium lattice constant of this compound is in good agreement with the available experimental and theoretical data reported in the literatures. The independent elastic constants (C_{11} , C_{12} , and C_{44}), bulk modulus B and its pressure derivatives B' , compressibility β , shear modulus G , Young's modulus Y , Poisson's ratio ν , and Lamé constants (μ, λ) are obtained and analyzed in comparison with the available theoretical and experimental data for both the singlecrystalline and polycrystalline BaHfO₃. The band structure calculations show that BaHfO₃ is a indirect bandgap material (R- Γ = 3.11 eV) derived basically from the occupied O 2*p* and unoccupied Hf 5*d* states, and it still awaits experimental confirmation. The density of states (total, site-projected, and *l*-decomposed) and the bonding charge density calculations make it clear that the covalent bonds exist between the Hf and O atoms and the ionic bonds exist between the Ba atoms and HfO₃ ionic groups in BaHfO₃. From our calculations, it is shown that BaHfO₃ should be promising as a candidate for synthesis and design of superhard materials due to the covalent bonding between the transition metal Hf 5*d* and O 2*p* states.

PACS numbers: 31.15.A-, 31.15.ae, 87.19.rd

Submitted to: *J. Phys.: Condens. Matter*

‡ Corresponding author.

1. Introduction

The perovskite-type oxides have the potential to be attractive functional materials because they have a wide range of interesting physical properties which have been extensively reported, such as ferroelectricity [1, 2, 3], semiconductivity [4], superconductivity [5], catalytic activity [6], piezoelectricity [7, 8], colossal magnetoresistance [9, 10], and thermoelectricity [6, 11]. Up to now, the perovskite-type oxides have been widely used in many fields, including spintronic devices, optical wave guides, laser-host crystals, high temperature oxygen sensors, surface acoustic wave devices, non-volatile memories, dynamic random access memories, frequency doublers, piezoelectric actuator materials, catalyst electrodes in certain types of fuel cells, and high- κ capacitors in various applications [12, 13].

The perovskite-type alkaline earth hafnate, BaHfO₃ belongs to the family of the perovskite-type oxides ABO₃ and is assigned to the pseudocubic cell of the perovskite structure, where A and B cations are in 12-fold and 6-fold coordination, respectively. More specifically, a Ba atom sits at cube corner position (0, 0, 0), a Hf atom sits at body centre position (1/2, 1/2, 1/2), and three O atoms sit at face centred positions (1/2, 1/2, 0) forming a regular octahedron, as depicted in Figure 1. There are few reported experimental studies devoted to this compound. Very recently, a polycrystalline sample of BaHfO₃ has been successfully prepared and some physical properties of this compound have been investigated[14].

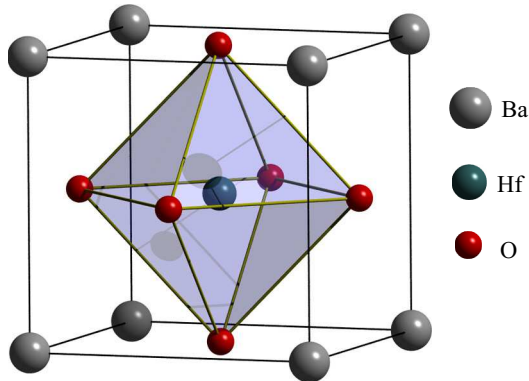


Figure 1: (Color online) The crystal structural perspective polyhedral view of the cubic perovskite-type BaHfO₃.

A more complete understanding of the physical properties of BaHfO₃ is prerequisite to the eventual technological applications of this compound. A systematic theoretical investigations of the structural, elastic and electronic properties of BaHfO₃ is necessary. As far as we know, there is surprisingly little theoretical work exploring its physical properties [15, 16, 17].

In this paper, we report a systematic study of the structural, elastic, and electronic properties of the cubic perovskite BaHfO₃, using the state-of-the-art pseudo-potential plane-waves (PP-PW) approach based on density functional theory (DFT) with revised

Perdew-Burke-Ernzerhof functional of the generalized gradient approximation (GGA-RPBE). Our studies have been motivated by the following reasons.

Even though the mentioned experimental and theoretical results [14, 15, 16, 17] for BaHfO₃ have been published, some results are still controversial and remain open problems. In the calculation of bulk modulus by Bouhemadou *et al* [16], a uniform P - V data set was used to fit to the third order Birch-Murnaghan equation [18], which would give inaccurate results. The calculated bandgap results of BaHfO₃ by Xiao *et al* [17] and Bouhemadou *et al* [16] are incompatible. Theoretical investigations of the bonding charge densities properties of BaHfO₃ hasn't been done. Therefore, based on DFT-GGA-RPBE method, we calculated the bulk modulus by using a dense sampling technology in the low-pressure region, the band structures, density of states (total, site-projected, and l-decomposed) and the bonding charge densities. It allows us to understand and clarify the uncertainties in comparison with other experimental and theoretical results [14, 15, 16, 17].

Elastic behavior for cubic perovskite BaHfO₃ is of great interest for its potential applications. Therefore, we have predicted the elastic parameters from accurate first principles DFT-GGA-RPBE calculations not only for BaHfO₃ monocrystal but also for its polycrystalline state, as this material has been prepared as polycrystalline samples [14, 19]. In this study, a set of physical parameters of monocrystalline BaHfO₃, such as optimized lattice parameter, elastic constants C_{11} , C_{12} , and C_{44} , bulk modulus B , compressibility β , and shear modulus G , is calculated, and the numerical estimates of the bulk modulus B , compressibility β , and shear modulus G , Young's modulus Y , Poisson's ratio (ν), and Lamé constants (μ, λ) of the polycrystalline BaHfO₃ (in the framework of the Voigt-Reuss-Hill approximation) are obtained and analyzed.

This paper is organized as follows: In Section 2 we briefly described the computational techniques used in the present work. Results and discussions of the structural, elastic, and electronic properties will be presented in Section 3. Finally, conclusions and remarks are given in Section 4.

2. Computational details

In this paper, all calculations are performed with the Cambridge Serial Total Energy Package (CASTEP) code [20], which is a implementation in pseudo-potential plane-waves (PP-PW) based density functional theory (DFT). The exchange-correlation potential is treated with the GGA-RPBE functional, developed by Hammer *et al* [21]. Coulomb potential energy caused by electron-ion interaction is described using Vanderbilt-type ultrasoft scheme [22, 23, 24]. The Ba $5s^2$, Ba $5p^6$, Ba $6s^2$, Hf $5d^2$, Hf $6s^2$, O $2s^2$, and O $2p^6$ electrons are treated as valence electrons for performing the pseudo atomic calculation. A 380 eV energy cut-off for the plane-wave basis and a (8, 8, 8) mesh in the Monkhorst-Pack scheme for the Brillouin-zone sampling are adopted during structure optimization. Atomic positions of BaHfO₃ are relaxed and optimized with a density mixing scheme using the Broyden-Fletcher-Goldfarb-Shanno

(BFGS) minimization technique. The following convergence criterions are reached: energy change per atom less than 2×10^{-6} eV, residual force less than 0.01 eV/Å, stress below 0.05 GPa, and the displacement of atoms during the geometry optimization less than 5×10^{-4} Å.

With the equilibrium geometry configuration, we applied the so-called stress-strain method to obtain the elastic constants in which the stress can be easily obtained within the density functional based electronic structure method [25]. The stress-strain relation can be described as [26]

$$(\sigma_1, \sigma_2, \sigma_3, \sigma_4, \sigma_5, \sigma_6) = C(\varepsilon_1, \varepsilon_2, \varepsilon_3, \varepsilon_4, \varepsilon_5, \varepsilon_6)^T, \quad (1)$$

where C is the elastic stiffness matrix. For the cubic crystal, there are only three non-zero independent symmetry elements (C_{11} , C_{12} , and C_{44}), each of which represents three equal elastic constants ($C_{11}=C_{22}=C_{33}$; $C_{12}=C_{23}=C_{31}$; $C_{44}=C_{55}=C_{66}$) [27]. A single strain with non-zero first and fourth components can give stresses relating to all three of these coefficients, yielding a very efficient method for obtaining elastic constants for the cubic system.

3. Results and discussions

3.1. Lattice constants

First, the equilibrium lattice constants (a_0) for the ideal stoichiometric perovskite BaHfO₃ was calculated. The results are listed in Table 1, along with the available experimental and theoretical data. As can be seen, our calculated equilibrium lattice parameter (a_0) is in excellent agreement with the experimental data and previous calculations: the calculated lattice constant deviates from the measured and the calculated ones within 2.8% and 0.8% respectively. The above results also show that the computational methods and parameters used in this paper are reasonable.

3.2. Elastic properties

Within the framework of the DFT-GGA-RPBE calculations, the values of elastic constants C_{ij} for BaHfO₃ are presented in Table 1. These three independent elastic constants in a cubic symmetry (C_{11} , C_{12} , and C_{44}) were estimated by calculating the stress tensors on applying strains to an equilibrium structure. All C_{ij} constants for BaHfO₃ crystal are positive and satisfy the generalized criteria [28, 29, 30] for mechanically stable crystals: $(C_{11}-C_{12})>0$, $(C_{11}+2C_{12})>0$, and $C_{44} >0$.

Considering that the above elastic parameters are obtained from first-principles calculations of BaHfO₃ monocystal. However, this material has been prepared as polycrystalline structure, [14, 19] and, therefore, it is useful to evaluate the corresponding parameters for the polycrystalline samples. For this purpose we have utilized the Voigt-Reuss-Hill (VRH) approximation [29]. In this approach, the actual effective modulus for polycrystals could be approximated by the arithmetic mean of the

Table 1: The lattice parameter (a_0 , in Å), elastic constants (C_{ij} , in GPa), bulk modulus (B , in GPa) and its pressure derivatives (B'), compressibility (β , in GPa^{-1}), shear modulus (G , in GPa), Young's modulus (Y , in GPa), Poisson's ratio (ν), and Lamé constants (μ, λ) for BaHfO_3 .

Parameters	Present work	Experimental	Other calculations
a_0	4.2858	4.171 ^a 4.17 ^c	4.2499 ^b 4.310 ^d
C_{11}	313.18	—	422 ^b 317.5 ^d
C_{12}	63.49	—	80 ^b 26.6 ^d
C_{44}	70.33	—	73 ^b 74.3 ^d
B	146.72 ^e 145.50 ^f	—	194 ^{b,e} 186 ^{b,f} 123.6 ^{d,e}
B'	5.08 ^f	—	5.02 ^{b,f}
β	6.82×10^{-3e} 6.87×10^{-3f}	8.78×10^{-3a}	—
G	88.68 ^e	79.5 ^a	97.6 ^d
Y	221.42 ^e	194 ^a	—
ν	0.2485	—	—
μ	88.68	—	—
λ	87.60	—	—

^a Reference [14].

^b Reference [16].

^c Reference [31].

^d Reference [17].

^e Obtained from the Voigt-Reuss-Hill (VRH) approximation [29].

^f Obtained from fitting the third-order Birch-Murnaghan equation [18].

two well-known bounds for monocrystals according to Voigt [32] and Reuss [33]. Then, the main mechanical parameters for cubic perovskite BaHfO_3 , namely, bulk modulus (B), compressibility (β), shear modulus (G), Young's modulus (Y), Poisson's ratio (ν), and Lamé constants (μ, λ) in the two mentioned approximations, Voigt (V) [32] and Reuss (R) [33], are calculated from the elastic constants of single crystal BaHfO_3 according to the following formulae [34, 35]:

$$\begin{aligned}
 B_{\text{V,R,VRH}} &= (C_{11} + 2C_{12}) / 3, \\
 G_{\text{V}} &= (C_{11} - C_{12} + 3C_{44}) / 5, \\
 G_{\text{R}} &= 5 / [4(S_{11} - S_{12}) + 3S_{44}]
 \end{aligned}
 \tag{2a}$$

$$\begin{aligned} &= 5(C_{11} - C_{12})C_{44}/[4C_{44} + 3(C_{11} - C_{12})], \\ G_{\text{VRH}} &= (G_{\text{V}} + G_{\text{R}})/2. \end{aligned} \quad (2b)$$

$$Y_{\text{VRH}} = 9G_{\text{VRH}}B_{\text{VRH}}/(G_{\text{VRH}} + 3B_{\text{VRH}}). \quad (2c)$$

$$\nu = (3B_{\text{VRH}} - 2G_{\text{VRH}})/[2(3B_{\text{VRH}} + G_{\text{VRH}})]. \quad (2d)$$

$$\begin{aligned} \mu &= Y_{\text{VRH}}/[2(1+\nu)], \\ \lambda &= \nu Y_{\text{VRH}}/[(1+\nu)(1-2\nu)]. \end{aligned} \quad (2e)$$

Where S in (2b) is the elastic compliance matrix, which is equal to the inverse of the elastic stiffness matrix C in (1).

The calculated values of the elastic parameters for the polycrystalline BaHfO₃ are given in Table 1. Our calculated elastic parameters are in reasonably good agreement with most of the available experimental data. The calculated large Bulk Modulus indicates a relative high incompressibility and hardness of BaHfO₃ according to the strong correlation between the bulk modulus and hardness of materials [36], implying that BaHfO₃ should be promising as a candidate for synthesis and design of superhard materials.

In order to further validate the reliability and accuracy of our calculated elastic constants for BaHfO₃, the calculated unit cell volumes under a series of applied hydrostatic pressures were used to construct the P - V data set, which was subsequently fitted to a third-order Birch-Murnaghan equation [18] (Figure 2):

$$P = \frac{3B}{2} \left[\left(\frac{V_0}{V} \right)^{7/3} - \left(\frac{V_0}{V} \right)^{5/3} \right] \left\{ 1 + \frac{3}{4}(B' - 4) \left[\left(\frac{V_0}{V} \right)^{2/3} - 1 \right] \right\}, \quad (3)$$

where V_0 is the the primitive unit cell's volume of BaHfO₃ determined from the zero pressure, B_0 is the bulk modulus and B' is its pressure derivative at zero pressure.

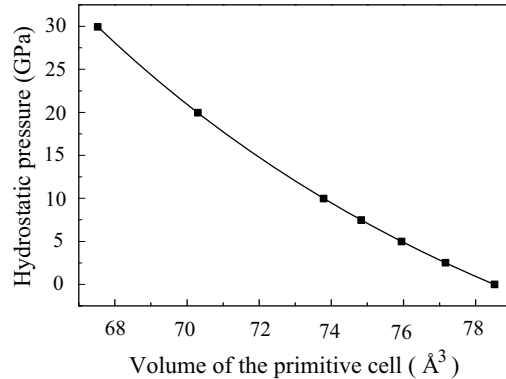


Figure 2: The calculated pressure-volume relation for BaHfO₃. The solid line is given by the third-order Birch-Murnaghan equation of state.

Considering that the values of B and B' determined by the equation of state (EOS) fitting process depend on the pressure range used in the calculations. Experimental values obtained using a diamond anvil cell are usually in the range 0~30 GPa, so this

pressure range is adopted by the present work. In addition, more accurate sampling in the low-pressure region is used to obtain an accurate value of the bulk modulus.

We obtained, by least-squares fitting of the non-uniform P - V data set to the third-order Birch-Murnaghan equation [18], the bulk modulus B_0 and its pressure derivative B' at zero pressure. The calculated results are listed in Table 1. Comparing the value from the Voigt-Reuss-Hill (VRH) approximation [29], our result is more accurate than that by Bouhemadou *et al* [16].

3.3. Electronic properties

The electronic band structure, density of states (total, site-projected, and l -decomposed) and bonding charge density which have been calculated for the equilibrium geometry of BaHfO₃ are shown in Figure 3, Figure 4 and Figure 5, respectively.

The calculated energy band structure of BaHfO₃ along the high symmetry lines in the first Brillouin zone is shown in Figure 3. The Fermi level E_F is chosen to locate at 0 eV and coincides with the top of the valence band. The valence band maximum (VBM) and conduction band minimum (CBM) are found to be 0 eV at R point and 3.11 eV at Γ point, respectively, indicating that this compound is a indirect bandgap material (R- Γ). These results are in good agreement with those obtained by Xiao *et al* [17], but inconsistent with those by Bouhemadou *et al* [16]. Considering that no experimental bandgap data for BaHfO₃ are available, the experimental studies are necessary to further testify the theoretical results. The values of the main band gaps and the width of the valence band obtained in the present work along with other theoretical results of the band structure for this compound are given in Table 2.

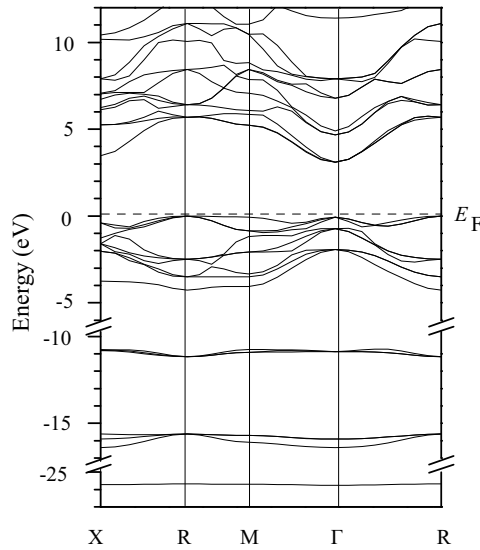


Figure 3: Band structure for BaHfO₃ along the high symmetry lines of the Brillouin zone, Fermi level $E_F=0$ eV.

Table 2: Electron band eigenvalues for the lowest conduction bands and the upper valence band widths of the BaHfO₃ (all of the energies are in eV).

Band structure features	This work	Other calculations
Direct		
Γ-Γ	3.17	2.99 ^a
M-M	5.30	5.61 ^a
R-R	5.76	5.87 ^a
X-X	3.87	3.80 ^a
Indirect		
Γ-M	5.30	5.50 ^a
Γ-R	5.82	5.83 ^a
Γ-X	3.54	3.42 ^a
M-Γ	3.17	—
R-Γ	3.11	3.1 ^b
X-Γ	3.49	—
Total-valence bandwidth	25.95	—

^a Reference [16].

^b Reference [17].

The total, site-projected, and *l*-decomposed densities of states (DOS) for BaHfO₃ are presented in Figure 4. The results are consistent with other theoretical studies [16, 17]. The Fermi level (E_F) and the conduction band minimum (CBM) are located close to peaks provided mainly by O 2*p* electrons and Hf 5*d* electrons, respectively. The lowest region of the valence band situated in the range from -25.95 to -25.46 eV is due to the Ba 6*s* states. The valence band which extend from -16.59 up to -15.36 eV is derived basically from the O 2*s* states with some mixing of Hf 6*s*, Hf 5*d*, and Ba 5*p* states. The valence band situated in the region from -11.39 up to -10.51 eV is essentially dominated by Ba 5*p* states, with admixture from O 2*s* states. The upper valence band (between -4.47 and 0 eV) is mainly due to O 2*p* states hybridized with some Hf 5*d* electrons, which suggests covalent bonding contributions in BaHfO₃. Here Hf 5*d* and O 2*p* orbitals overlap, resulting in covalent bonding between the Hf and O atoms in this material. The Hf-O covalency will also responsible for the hardness of this compound [37]. The lower conduction bands are contributed mainly by Hf 5*d*, Ba 5*d*, and Ba 6*s* states.

The bonding charge density is an useful tool to describe the redistribution of the electrons along with the bonding process. In order to interpret the bonding mechanism of BaHfO₃, the bonding-charge density was used to study the bonding characteristics of this compound. The bonding charge density is defined as the difference between the total charge density in the solid and the superposition of neutral atomic charge densities

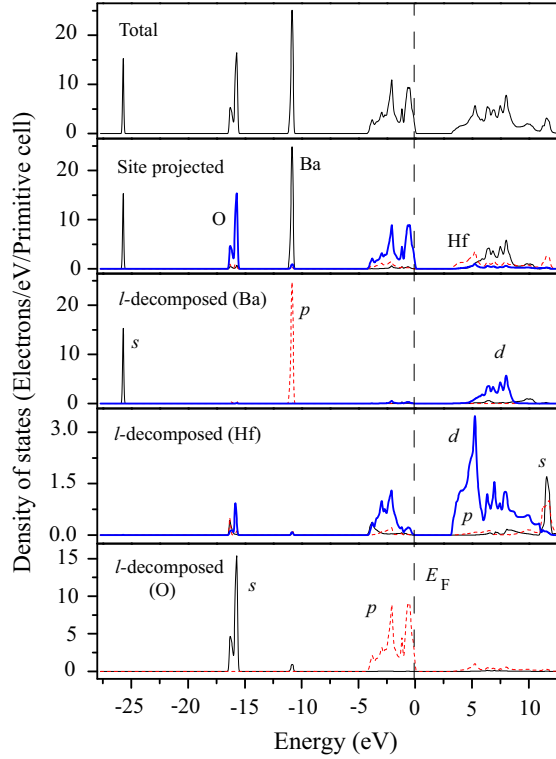


Figure 4: (Color online) Total, site-projected, and l -decomposed DOS for BaHfO_3 . The black (thin), red (dashed), and blue (thick) lines represent the Ba, Hf, and O atoms' DOS contributions in the site-projected case and the s , p , and d orbitals' DOS contributions in the l -decomposed case, respectively, Fermi level $E_F=0$ eV.

placed at the same atomic sites, with the formula as below [38]:

$$\Delta\rho(r) = \rho_{solid}(r) - \sum_{\alpha} \rho_{\alpha}(r - r_{\alpha}), \quad (4)$$

where $\rho_{solid}(r)$ is the total charge density of the equilibrium structure and $\rho_{\alpha}(r - r_{\alpha})$ is the charge density of the neutral atom α . Therefore, the bonding charge density represents the net charge redistribution as atoms are brought together to form the crystal.

The bonding-charge densities in the (100) and (110) plane of BaHfO_3 have been calculated and shown in Figure 5(a) and (b), with solid and dashed contour lines denoting positive (hence accumulation) and negative (hence depletion) of electron density, respectively, relative to the atomic electron density. The positive (negative) charge redistribution can be identified with electronic transfer into (outward) bonding or anti-bonding electronic states.

As shown in Figure 5, Ba atoms have more anti-bonding charge density in the (100) plane than that in the (110) plane. Moreover in the (110) plane, the electrons accumulate and distribute along the Hf-O bond and deflect to bonding line, resulting in strong covalent characteristics of the Hf-O bond, which coincides well with the results obtained from the densities of states (DOS) analysis. The covalent characteristics of the Hf-O bond will also result in a high hardness value and can contribute to the

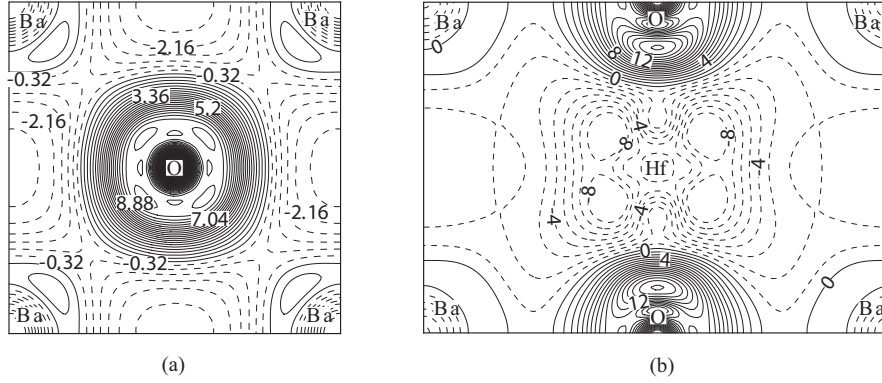


Figure 5: The bonding charge densities for BaHfO₃: (a) in the (100) plane and (b) in the (110) plane. The contour step size is 0.46 e/f.u. and 1 e/f.u. for (a) and (b), respectively, where f.u. denotes formula unit.

elastic incompressibility (bulk modulus) of this material, which are consistent with the corresponding results obtained from the elastic properties and density of states (DOS) calculations, as well as the experimental data [14]. The electrons depletion process occurs near the Ba atoms both in the (100) and (110) planes could be ascribed to the presence of the strong ionic characteristics between the Ba atoms and HfO₃ ionic groups.

4. Conclusions

The structural, elastic, and electronic properties of the cubic perovskite BaHfO₃ have been studied by using the density functional theory with the GGA-RPBE approximation. Our main results and conclusions can be summarized as follows:

(i) The calculated equilibrium lattice constant of this compound is in good agreement with the available experimental and theoretical data reported in the literatures.

(ii) We have used a dense sampling technology in the low-pressure region to obtain an accurate value of the bulk modulus by fitting the third-order Birch-Murnaghan equation [18]. Comparing the value from the Voigt-Reuss-Hill (VRH) approximation [29], our result is more accurate than that by Bouhemadou *et al* [16].

(iii) The electronic structure calculations showed that BaHfO₃ is an indirect bandgap material ($R-\Gamma = 3.11$ eV). This result is consistent with the result by Xiao *et al* [17], but differs from that by Bouhemadou *et al* [16]. Considering that no experimental bandgap data for BaHfO₃ are available, the experimental studies are necessary to further testify the theoretical results.

(iv) The calculated elastic properties, including bulk modulus (B) and its pressure derivatives (B'), compressibility (β), shear modulus (G), Young's modulus (Y), Poisson's ratio (ν), and Lamé constants (μ, λ), are in reasonably good agreement with the available experimental data.

(v) Analyses of the density of states (total, site-projected, and l -decomposed)

revealed that the lower conduction bands are contributed mainly by Hf 5*d*, Ba 5*d*, and 6*s* states, while in the valence region, the Hf 5*d* states are partially hybridized with O 2*p* and located below the near-Fermi bands formed predominantly by O 2*p* states. The bonding charge density calculations give further evidence that the covalent bonds exist between the Hf and O atoms and the ionic bonds exist between the Ba atoms and HfO₃ ionic groups in BaHfO₃.

Acknowledgments

This work was supported by the National Nature Science Foundation of China (No. O311011301) and the Knowledge Innovation Program of the Chinese Academy of Sciences (No. 072C201301). The authors thank the Shanghai Supercomputer Center and the Center for High Performance Computing, Northwestern Polytechnical University, from where the computational work in this paper was done and the technical support was given.

References

- [1] Samantaray C B and Sim H and Hwang H. Electronic structure and optical properties of barium strontium titanate (Ba_{*x*}Sr_{1-*x*}TiO₃) using first-principles method. *Phys. B: Condens. Matter*, 351(1-2):158, 2004.
- [2] Bednorz J G and Müller K A. Sr_{1-*x*}Ca_{*x*}TiO₃: An XY Quantum Ferroelectric with Transition to Randomness. *Phys. Rev. Lett.*, 52(25):2289, 1984.
- [3] Samantaray C B and Sim H and Hwang H. The electronic structures and optical properties of BaTiO₃ and SrTiO₃ using first-principles calculations. *Microelectron. J.*, 36(8):725, 2005.
- [4] Frederikse H P R and Thurber W R and Hosler W R. Electronic Transport in Strontium Titanate. *Phys. Rev.*, 134(2A):A442, 1964.
- [5] Koonce C S and Cohen M L and Schooley J F and Hosler W R and Pfeiffer E R. Superconducting Transition Temperatures of Semiconducting SrTiO₃. *Phys. Rev.*, 163(2):380, 1967.
- [6] Henrich V E. The surfaces of metal oxides. *Rep. Prog. Phys.*, 48(11):1481, 1985.
- [7] Wang H and Wang B and Li Q and Zhu Z and Wang R and Woo C H. First-principles study of the cubic perovskites BiMO₃ (M = Al, Ga, In, and Sc). *Phys. Rev. B*, 75(24):245209, 2007.
- [8] Baettig P and Schelle C F and LeSar R and Waghmare U V and Spaldin N A. Theoretical Prediction of New High-Performance Lead-Free Piezoelectrics. *Chem. Mater.*, 17(6):1376, 2005.

- [9] Millis A J and Shraiman B I and Mueller R. Dynamic Jahn-Teller Effect and Colossal Magnetoresistance in $\text{La}_{1-x}\text{Sr}_x\text{MnO}_3$. *Phys. Rev. Lett.*, 77(1):175, 1996.
- [10] Colossal Magnetoresistive Oxides (Advances in Condensed Matter Science, Volume 2). CRC, 1 edition, 2000.
- [11] Muta H and Kurosaki K and Yamanaka S. Thermoelectric properties of rare earth doped SrTiO_3 . *J. Alloys Compd.*, 350(1-2):292, 2003.
- [12] Mete E and Shaltaf R and Ellialtıođlu, Ő. Electronic and structural properties of a 4d perovskite: Cubic phase of SrZrO_3 . *Phys. Rev. B*, 68(3):035119, 2003.
- [13] Henrich V E and Cox P A. *The surface science of metal oxides*. Cambridge University Press, Cambridge ; New York, 1994.
- [14] Maekawa T and Kurosaki K and Yamanaka S. Thermal and mechanical properties of perovskite-type barium hafnate. *J. Alloys Compd.*, 407(1-2):44, 2006.
- [15] Kitamura M and Chen H. Electronic structure calculations of perovskite-type oxides using the self-consistent-charge extended Huckel tight-binding method. *Ferroelectrics*, 210(1):13, 1998.
- [16] Bouhemadou A and Djabi F and Khenata R. First principles study of structural, elastic, electronic and optical properties of the cubic perovskite BaHfO_3 . *Phys. Lett. A*, 372(24):4527, 2008.
- [17] Xiao Y and Xiao-Guang L and Gui-Feng C and Jun S and Yang-Xian L. First principle calculation of structural, elastic and electronic properties of XHfO_3 (X=Ba, Sr). *Acta Phys Sin-Ch Ed*, 56(9):5366, 2007.
- [18] Poirier J-P. *Introduction to the Physics of the Earth's Interior (Cambridge Topics in Mineral Physics and Chemistry)*. Cambridge University Press, 1991.
- [19] Zhang J L and Evetts J E. Preparation of BaHfO_3 , using a spray drying method. *Mater. Lett.*, 15:331, 1993.
- [20] Segall M D and Lindan P J D and Probert M J and Pickard C J and Hasnip P J and Clark S J and Payne M C. First-principles simulation: ideas, illustrations and the CASTEP code. *J. Phys.: Condens. Matter*, (11):2717, 2002.
- [21] Hammer B and Hansen L B and Nørskov J K. Improved adsorption energetics within density-functional theory using revised Perdew-Burke-Ernzerhof functionals. *Phys. Rev. B*, 59(11):7413, 1999.
- [22] Laasonen K and Car R and Lee C and Vanderbilt D. Implementation of ultrasoft pseudopotentials in ab initio molecular dynamics. *Phys. Rev. B*, 43(8):6796, 1991.
- [23] Laasonen K and Pasquarello A and Car R and Lee C and Vanderbilt D. Car-Parrinello molecular dynamics with Vanderbilt ultrasoft pseudopotentials. *Phys. Rev. B*, 47(16):10142, 1993.
- [24] Vanderbilt D. Soft self-consistent pseudopotentials in a generalized eigenvalue formalism. *Phys. Rev. B*, 41(11):7892, 1990.
- [25] Nielsen O H and Martin R M. Stresses in semiconductors: Ab initio calculations on Si, Ge, and GaAs. *Phys. Rev. B*, 32(6):3792, 1985.

- [26] Fan C Z and Zeng S Y and Li L X and Zhan Z J and Liu R P and Wang W K and Zhang P and Yao Y G. Potential superhard osmium dinitride with fluorite and pyrite structure: First-principles calculations. *Phys. Rev. B*, 74(12):125118, 2006.
- [27] Nye J F. *Physical properties of crystals : their representation by tensors and matrices*. Clarendon, Oxford, 1985.
- [28] Yip S and Li J and Tang M and Wang J. Mechanistic aspects and atomic-level consequences of elastic instabilities in homogeneous crystals. *Mater. Sci. Eng., A*, 317(1-2):236, 2001.
- [29] Grimvall G. *Thermophysical Properties of Materials (Selected Topics in Solid State Physics, No 18)*. North-Holland, 1986.
- [30] Wang J and Yip S and Phillpot S R and Wolf D. Crystal instabilities at finite strain. *Phys. Rev. Lett.*, 71(25):4182, 1993.
- [31] López Garcíá A R and de la Presa P and Rodríguez A M. Temperature dependence of the hyperfine interaction in the cubic phase of BaHfO₃. *Phys. Rev. B*, 44(17):9708, 1991.
- [32] Voigt W. *Lehrbuch Der Kristallphysik*. Johnson Reprint Corp, 1928.
- [33] Reuss A. Berechnung der Fließ grenze von Mischkristallen auf Grund der Plastizitätsbedingung für Einkristalle. *Z. Angew. Math. Mech.*, 9(1):49, 1929.
- [34] Anderson O L. A simplified method for calculating the debye temperature from elastic constants. *J. Phys. Chem. Solids*, 24(7):909, 1963.
- [35] Schreiber E and Anderson O L and Soga N. *Elastic constants and their measurement*. McGraw-Hill, New York, 1973.
- [36] Haines J and Leger J M and Bocquillon G. Synthesis and design of superhard materials. *Annu. Rev. Mater. Res.*, 31:1, 2001.
- [37] Jhi S-H and Ihm J and Louie S G and Cohen M L. Electronic mechanism of hardness enhancement in transition-metal carbonitrides. *Nature*, 399(6732):132, 1999.
- [38] Sun S N and Kioussis N and Lim S-P and Gonis A and Gourdin W H. Impurity effects on atomic bonding in Ni₃Al. *Phys. Rev. B*, 52(20):14421, 1995.